Research Article | Vol. 7, No. 7 | 1 Jul 2017 | OPTICAL MATERIALS EXPRESS 2682
Optical Materials EXPRESS

Large-scale synthesis of ZnO nanoparticles and their application as phosphors in light-emitting devices

KAI-KAI LIU,[1,2] CHONG-XIN SHAN,[1,3,*] RUI ZHOU,[3] QI ZHAO,[3] AND DE-ZHEN SHEN[1]

[1]*State Key Laboratory of Luminescence and Applications, Changchun Institute of Optics, Fine Mechanics and Physics, Chinese Academy of Sciences, Changchun 130033, China*
[2]*University of Chinese Academy of Sciences, Beijing 100049, China*
[3]*School of Physics and Engineering, No. 75 Daxue Road, Zhengzhou University, Zhengzhou 450052, China*
**shancx@ciomp.ac.cn*

Abstract: A simple one-pot route to large-scale synthesis of ZnO nanoparticles (NPs) has been demonstrated, and the ZnO NPs can be produced more than 34 grams in one synthesis process. The ZnO NPs show bright yellowish fluorescence under ultraviolet illumination with a quantum yield (QY) of 42%, which make them suitable for application as phosphors in light-emitting devices (LEDs). Yellowish LEDs have been fabricated by employing the ZnO NP powder as phosphors, and the luminous efficiency of the LEDs can reach 64.2 lm/W. Additionally, the fluorescence intensity of the phosphors shows little degradation when the ambient temperature reaches 100 °C, and the correlated color temperature of the LEDs remains constant when the driving current reaches 100 mA, indicating the good temperature and injection-current stability of the ZnO NP phosphors.

OCIS codes: (160.4236) Nanomaterials; (160.4670) Optical materials; (160.4760) Optical properties; (230.3670) Light-emitting diodes.

References and links

1. Y. J. Lu, Z. F. Shi, C. X. Shan, and D. Z. Shen, "ZnO-based deep-ultraviolet light-emitting devices," Chin. Phys. B 26(4), 047703 (2017).
2. X. Li, Y. Liu, X. Song, H. Wang, H. Gu, and H. Zeng, "Intercrossed carbon nanorings with pure surface states as low-cost and environment-friendly phosphors for white-light-emitting diodes," Angew. Chem. Int. Ed. Engl. **54**(6), 1759–1764 (2015).
3. J. W. Moon, J. S. Kim, B. G. Min, H. M. Kim, and J. S. Yoo, "Optical characteristics and longevity of quantum dot-coated white LED," Opt. Mater. Express **4**(10), 2174 (2014).
4. Y. Q. Li, A. Rizzo, R. Cingolani, and G. Gigli, "Bright White-Light-Emitting Device from Ternary Nanocrystal Composites," Adv. Mater. **18**(19), 2545–2548 (2006).
5. J. Hye Oh, S. Ji Yang, and Y. Rag Do, "Healthy, natural, efficient and tunable lighting: four-package white LEDs for optimizing the circadian effect, color quality and vision performance," Light Sci. Appl. **3**(2), e141 (2014).
6. F. Zhang, X. Feng, Y. Zhang, L. Yan, Y. Yang, and X. Liu, "Photoluminescent carbon quantum dots as a directly film-forming phosphor towards white LEDs," Nanoscale **8**(16), 8618–8632 (2016).
7. Q. Qiao, B. H. Li, C. X. Shan, J. S. Liu, J. Yu, X. H. Xie, Z. Z. Zhang, T. B. Ji, Y. Jia, and D. Z. Shen, "Light-emitting diodes fabricated from small-size ZnO quantum dots," Mater. Lett. 74, 104- 106 (2012).
8. T. Pulli, T. Dönsberg, T. Poikonen, F. Manoocheri, P. Kärhä, and E. Ikonen, "Advantages of white LED lamps and new detector technology in photometry," Light Sci. Appl. **4**(9), e332 (2015).
9. X. Wang, X. Yan, W. Li, and K. Sun, "Doped quantum dots for white-light-emitting diodes without reabsorption of multiphase phosphors," Adv. Mater. **24**(20), 2742–2747 (2012).
10. S. K. Panda, S. G. Hickey, H. V. Demir, and A. Eychmüller, "Bright white-light emitting manganese and copper co-doped ZnSe quantum dots," Angew. Chem. Int. Ed. Engl. **50**(19), 4432–4436 (2011).
11. C. C. Lin, W.-T. Chen, C.-I. Chu, K.-W. Huang, C.-W. Yeh, B.-M. Cheng, and R.-S. Liu, "UV/VUV switch-driven color-reversal effect for Tb-activated phosphors," Light Sci. Appl. **5**(4), e16066 (2016).
12. J. Huang, X. Hu, J. Shen, D. Wu, C. Yin, R. Xiang, C. Yang, X. Liang, and W. Xiang, "Facile synthesis of a thermally stable Ce^{3+}:$Y_3Al_5O_{12}$ phosphor-in-glass for white LEDs," CrystEngComm **17**(37), 7079–7085 (2015).

#292445 https://doi.org/10.1364/OME.7.002682
Journal © 2017 Received 7 Apr 2017; revised 21 May 2017; accepted 23 May 2017; published 29 Jun 2017

Optical Materials EXPRESS

13. J. Ziegler, S. Xu, E. Kucur, F. Meister, M. Batentschuk, F. Gindele, and T. Nann, "Silica-Coated InP/ZnS Nanocrystals as Converter Material in White LEDs," Adv. Mater. **20**(21), 4068–4073 (2008).
14. L. Wang, X. Wang, T. Kohsei, K. Yoshimura, M. Izumi, N. Hirosaki, and R.-J. Xie, "Highly efficient narrow-band green and red phosphors enabling wider color-gamut LED backlight for more brilliant displays," Opt. Express **23**(22), 28707–28717 (2015).
15. B. Wang, H. Lin, J. Xu, H. Chen, and Y. Wang, "CaMg2Al16O27:Mn4+-based Red Phosphor: A Potential Color Converter for High-Powered Warm W-LED," ACS Appl. Mater. Interfaces **6**(24), 22905–22913 (2014).
16. P. P. Dai, C. Li, X. T. Zhang, J. Xu, X. Chen, X. L. Wang, Y. Jia, X. Wang, and Y. C. Liu, "A single Eu2+-activated high-color-rendering oxychloride white-light phosphor for white-light-emitting diodes," Light Sci. Appl. **5**(2), e16024 (2016).
17. H. Zhu, C. C. Lin, W. Luo, S. Shu, Z. Liu, Y. Liu, J. Kong, E. Ma, Y. Cao, R. S. Liu, and X. Chen, "Highly efficient non-rare-earth red emitting phosphor for warm white light-emitting diodes," Nat. Commun. **5**, 4312 (2014).
18. H. Zhou, Q. Wang, and Y. Jin, "Temperature dependence of energy transfer in tunable white light-emitting phosphor BaY2Si3O10:Bi3+,Eu3+for near UV LEDs," J. Mater. Chem. C Mater. Opt. Electron. Devices **3**(42), 11151–11162 (2015).
19. L. Chen, C. Lai, R. Marchewka, R. M. Berry, and K. C. Tam, "Use of CdS quantum dot-functionalized cellulose nanocrystal films for anti-counterfeiting applications," Nanoscale **8**(27), 13288–13296 (2016).
20. B. C. Marin, S. W. Hsu, L. Chen, A. Lo, D. W. Zwissler, Z. Liu, and A. R. Tao, "Plasmon-Enhanced Two-Photon Absorption in Photoluminescent Semiconductor Nanocrystals," ACS Photonics **3**(4), 526–531 (2016).
21. C. Ma, M. Zhou, D. Wu, M. Feng, X. Liu, P. Huo, W. Shi, Z. Ma, and Y. Yan, "One-step hydrothermal synthesis of cobalt and potassium codoped CdSe quantum dots with high visible light photocatalytic activity," CrystEngComm **17**(7), 1701–1709 (2015).
22. P. Lu, D. Li, P. Zhang, D. Tan, W. Mu, J. Xu, W. Li, and K. Chen, "Time-resolved and temperature-dependent photoluminescence study on phosphorus doped Si quantum dots/SiO_2 multilayers with ultra-small dot sizes," Opt. Mater. Express **6**(10), 3233 (2016).
23. S. Bera, S. K. Maity, and D. Haldar, "Photoelectrochemical properties of CdSe quantum dots doped disk-like tripeptide capsule," CrystEngComm **16**(22), 4834–4841 (2014).
24. A. L. Rogach, N. Gaponik, J. M. Lupton, C. Bertoni, D. E. Gallardo, S. Dunn, N. Li Pira, M. Paderi, P. Repetto, S. G. Romanov, C. O'Dwyer, C. M. Sotomayor Torres, and A. Eychmüller, "Light-emitting diodes with semiconductor nanocrystals," Angew. Chem. Int. Ed. Engl. **47**(35), 6538–6549 (2008).
25. T. Aubert, S. J. Soenen, D. Wassmuth, M. Cirillo, R. Van Deun, K. Braeckmans, and Z. Hens, "Bright and stable CdSe/CdS@SiO_2 nanoparticles suitable for long-term cell labeling," ACS Appl. Mater. Interfaces **6**(14), 11714–11723 (2014).
26. Y. Chang, X. Yao, Z. Zhang, D. Jiang, Y. Yu, L. Mi, H. Wang, G. Li, D. Yu, and Y. Jiang, "Preparation of highly luminescent BaSO4protected CdTe quantum dots as conversion materials for excellent color-rendering white LEDs," J. Mater. Chem. C Mater. Opt. Electron. Devices **3**(12), 2831–2836 (2015).
27. N. A. Hamizi, F. Aplop, H. Y. Haw, A. N. Sabri, A. Y. Y. Wern, N. N. Shapril, and M. R. Johan, "Tunable optical properties of Mn-doped CdSe quantum dots synthesized via inverse micelle technique," Opt. Mater. Express **6**(9), 2915 (2016).
28. A. M. Derfus, W. C. W. Chan, and S. N. Bhatia, "Probing the Cytotoxicity of Semiconductor Quantum Dots," Nano Lett. **4**(1), 11–18 (2004).
29. R. Hardman, "A toxicologic Review of Quantum Dots: Toxicity Depends on Physicochemical and Environmental Factors," Environ. Health Perspect. **114**(2), 165–172 (2006).
30. D. X. Ye, Y. Y. Ma, W. Zhao, H. M. Cao, J. L. Kong, H. M. Xiong, and H. Möhwald, "ZnO-Based Nanoplatforms for Labeling and Treatment of Mouse Tumors without Detectable Toxic Side Effects," ACS Nano **10**(4), 4294–4300 (2016).
31. L. W. Sun, H. Q. Shi, W. N. Li, H. M. Xiao, S. Y. Fu, X. Z. Cao, and Z. X. Li, "Lanthanum-doped ZnO quantum dots with greatly enhanced fluorescent quantum yield," J. Mater. Chem. **22**(17), 8221–8227 (2012).
32. K. K. Liu, C. X. Shan, G. H. He, R. Q. Wang, L. Dong, and D. Z. Shen, "Rewritable Painting Realized from Ambient-Sensitive Fluorescence of ZnO Nanoparticles," Sci. Rep. **7**, 42232 (2017).
33. J. Kwak, W. K. Bae, D. Lee, I. Park, J. Lim, M. Park, H. Cho, H. Woo, D. Y. Yoon, K. Char, S. Lee, and C. Lee, "Bright and efficient full-color colloidal quantum dot light-emitting diodes using an inverted device structure," Nano Lett. **12**(5), 2362–2366 (2012).
34. B. S. Mashford, M. Stevenson, Z. Popovic, C. Hamilton, Z. Zhou, C. Breen, J. Steckel, V. Bulovic, M. Bawendi, S. Coe-Sullivan, and P. T. Kazlas, "High-efficiency quantum-dot light-emitting devices with enhanced charge injection," Nat. Photonics **7**(5), 407–412 (2013).
35. L. Qian, Y. Zheng, J. Xue, and P. H. Holloway, "Stable and efficient quantum-dot light-emitting diodes based on solution-processed multilayer structures," Nat. Photonics **5**(9), 543–548 (2011).
36. J. Pan, J. Chen, Q. Huang, Q. Khan, X. Liu, Z. Tao, Z. Zhang, W. Lei, and A. Nathan, "Size Tunable ZnO Nanoparticles To Enhance Electron Injection in Solution Processed QLEDs," ACS Photonics **3**(2), 215–222 (2016).
37. D. Y. Guo, C. X. Shan, S. N. Qu, and D. Z. Shen, "Highly sensitive ultraviolet photodetectors fabricated from ZnO quantum dots/carbon nanodots hybrid films," Sci. Rep. **4**(1), 7469 (2014).

Optical Materials EXPRESS

38. N. Nasiri, R. Bo, F. Wang, L. Fu, and A. Tricoli, "Ultraporous Electron-Depleted ZnO Nanoparticle Networks for Highly Sensitive Portable Visible-Blind UV Photodetectors," Adv. Mater. **27**(29), 4336–4343 (2015).
39. Y. J. Park, J. H. Yang, B. D. Ryu, J. Cho, T. V. Cuong, and C.-H. Hong, "Solution-processed multidimensional ZnO/CuO heterojunction as ultraviolet sensing," Opt. Mater. Express **5**(8), 1752 (2015).
40. P. K. Shrestha, Y. T. Chun, and D. Chu, "A high-resolution optically addressed spatial light modulator based on ZnO nanoparticles," Light Sci. Appl. **4**(3), e259 (2015).
41. H. M. Xiong, "ZnO nanoparticles applied to bioimaging and drug delivery," Adv. Mater. **25**(37), 5329–5335 (2013).
42. K. Matsuyama, N. Ihsan, K. Irie, K. Mishima, T. Okuyama, and H. Muto, "Bioimaging application of highly luminescent silica-coated ZnO-nanoparticle quantum dots with biotin," J. Colloid Interface Sci. **399**, 19–25 (2013).
43. Z. Y. Zhang, Y. D. Xu, Y. Y. Ma, L. L. Qiu, Y. Wang, J. L. Kong, and H. M. Xiong, "Biodegradable ZnO@polymer core-shell nanocarriers: pH-triggered release of doxorubicin in vitro," Angew. Chem. Int. Ed. Engl. **52**(15), 4127–4131 (2013).
44. X. Cai, Y. Luo, W. Zhang, D. Du, and Y. Lin, "pH-Sensitive ZnO Quantum Dots-Doxorubicin Nanoparticles for Lung Cancer Targeted Drug Delivery," ACS Appl. Mater. Interfaces **8**(34), 22442–22450 (2016).
45. N. Tripathy, R. Ahmad, H. A. Ko, G. Khang, and Y.-B. Hahn, "Enhanced anticancer potency using an acid-responsive ZnO-incorporated liposomal drug-delivery system," Nanoscale **7**(9), 4088–4096 (2015).
46. H. Ghorbani, F. Mehr, H. Pazoki, and B. Rahmani, "Synthesis of ZnO Nanoparticles by Precipitation Method," Oriental J. Chem. **31**(2), 1219–1221 (2015).
47. H. M. Xiong, D. P. Xie, X. Y. Guan, Y. J. Tan, and Y. Y. Xia, "Water-stable blue-emitting ZnO@polymer core?shell microspheres," J. Mater. Chem. **17**(24), 2490–2496 (2007).
48. H. Q. Shi, W. N. Li, L. W. Sun, Y. Liu, H. M. Xiao, and S. Y. Fu, "Synthesis of silane surface modified ZnO quantum dots with ultrastable, strong and tunable luminescence," Chem. Commun. (Camb.) **47**(43), 11921–11923 (2011).
49. S. Choi, M. R. Phillips, I. Aharonovich, S. Pornsuwan, B. C. C. Cowie, and C. Ton-That, "Photophysics of Point Defects in ZnO Nanoparticles," Adv. Opt. Mater. **3**(6), 821–827 (2015).
50. X. Xu, C. Xu, X. Wang, Y. Lin, J. Dai, and J. Hu, "Control mechanism behind broad fluorescence from violet to orange in ZnO quantum dots," CrystEngComm **15**(5), 977–981 (2013).
51. Y. Zhang, Y. Hu, J. Lin, Y. Fan, Y. Li, Y. Lv, and X. Liu, "Excitation Wavelength Independence: Toward Low-Threshold Amplified Spontaneous Emission from Carbon Nanodots," ACS Appl. Mater. Interfaces **8**(38), 25454–25460 (2016).
52. H. Zeng, G. Duan, Y. Li, S. Yang, X. Xu, and W. Cai, "Blue Luminescence of ZnO Nanoparticles Based on Non-Equilibrium Processes: Defect Origins and Emission Controls," Adv. Funct. Mater. **20**(4), 561–572 (2010).
53. D. Y. Guo, C. X. Shan, K. K. Liu, Q. Lou, and D. Z. Shen, "Surface plasmon effect of carbon nanodots," Nanoscale **7**(45), 18908–18913 (2015).

1. Introduction

Light-emitting devices (LEDs) have been considered next generation lighting source due to their merits of energy-conserving [1–3], long lifetime [4–6], high efficiency [7–9], etc. The current white LED technology is usually realized by coating yellow [10–12] or red and green [13–15] phosphors onto blue LED chips or coating tricolor phosphors onto ultraviolet (UV) LED chips [16–18]. Rare earth based phosphors play a dominant role in the mainstream phosphors market. However, the reserve abundance of rare earth elements on the earth is usually very limited, and the mining and purifying of rare earths usually cause severe pollution to both water and land. Thus, it is of great significance and importance to develop phosphors avoiding the use of rare earth elements.

In recent years, fluorescent semiconductor nanoparticles (NPs) have attracted much attention due to their unique optical properties like high efficiency, narrow emission band, tunable emission wavelength, and so on [19–22]. Among these NPs, CdSe and CdTe [23–27] are the most extensively investigated materials, but the toxicity and environmental pollution issues of these NPs limit their applications seriously [28, 29]. As one of the group II-VI semiconductors, ZnO NPs have been used for labeling [30–32], electron transport layer [33–36], detector [37–40], bioimaging [41, 42], drug delivery [43–45], etc., due to their high luminescent efficiency, eco-friendly, low-cost, and mild synthesis process [46]. However, none report on employing luminescent ZnO NPs as phosphors of LEDs can be found to date. The major reason lies in that the large-scale synthesis of luminescent ZnO NPs is still a challenge. ZnO NPs are usually synthesized by sol-gel method via hydrolysis of zinc salts in alcohol solution. However, some reports indicate that the ZnO NPs derived by traditional sol-

Optical Materials EXPRESS

gel method are unstable and tend to aggregate seriously [47, 48], which will lead to drastic decrease in fluorescence efficiency of the NPs. In addition, large-scale production of ZnO NPs, which is necessary for phosphors of LEDs, has not been reported yet. Therefore, it is urgently needed to develop a simple route to large-scale synthesis of luminescent ZnO NPs to meet the requirement of phosphors for application in LEDs.

In this paper, a route to large-scale synthesis of ZnO NPs has been demonstrated, and over 34 grams of ZnO NP powders can be realized in one synthesis process. The emission wavelength of the NPs is located at around 535 nm, and the quantum yields (QYs) of the NPs can reach 42%. The ZnO NP powders have been coated onto UV chip acting as phosphors, and the luminous efficiency of the ZnO NP powder coated LED can reach 64.2 lm/W, also the LED shows good temperature and injection-current stability, promising the capability of the ZnO NPs in application as phosphors in LEDs.

2. Experimental

2.1 Materials:

Zinc acetate dihydrate (Zn(Ac)2·2H2O, purity > 99%), potassium hydroxide (KOH, purity > 95%), 3-aminopropyltriethoxysilane (APTES, purity>98%) and ethanol (putiry > 99.9%) were used as reagents for the synthesis of ZnO NPs. All the reagents purchased from Aladdin. Note that all the chemical reagents are of analytical grade and used as-received without further purification.

2.2 Large-scale synthesis of ZnO NP powders:

The large-scale preparation procedure of the ZnO NP powders is as follows. First of all, 55 g (0.25 mol) $Zn(Ac)_2{\cdot}2H_2O$ was dissolved in 1.5 L ethanol solution and the solution was refluxed at 78 °C for 30 minutes under continuous stirring. Then 200 mL 1.75 M KOH ethanol solution was added into the $Zn(Ac)_2{\cdot}2H_2O$ ethanol under continuous stirring at 30 °C. The $Zn(Ac)_2{\cdot}2H_2O$ ethanol solution would become colorless and transparent after the injection of KOH ethanol solution, indicating that ZnO NPs have been formed. The NP processing is termination by the mixture of deionized water and APTES. Finally, 20 mL deionized water and 4 mL APTES mixture was added into the ZnO NPs ethanol solution until the solution became turbid. After that, the solution was centrifuged (6000 rpm, 2 minutes) and the obtained precipitations were washed using ethanol for several times to remove the unreacted precursors. The washed precipitation was then placed into an oven (80 °C) for 12 hours to form ZnO NP powders.

2.3 Coating ZnO NP powders onto UV chip:

For fabrication of the LED, polydimethylsiloxane (PDMS) were premixed with the ZnO NP phosphors with a mass ratio of 2:1. The mixture was dropped onto the UV chip. After that, the UV chip with ZnO NP phosphors was placed into an oven at 80°C for 1 hour to cure the PDMS.

2.4 Characterizations:

A JEM-2010 transmission electron microscope (TEM) and a Bruker D8 Discover (Germany) x-ray diffractometer (XRD) were used to characterize the structural properties of the ZnO NPs. The size of the NPs was characterized by Malvern Zetasizer Nano ZSP (United Kingdom). The bonding state of the ZnO NPs was measured using Thermo ESCALAB-250 x-ray photoelectron spectroscopy (XPS). The optical properties of the ZnO NPs were assessed in a Hitachi F-7000 spectrophotometer. The absorption spectra of the samples were acquired in a Shimadzu UV-3101PC spectrometer. The transient photoluminescence spectra of the ZnO NPs were recorded in a FLS-920 fluorescence spectrometer. The QY of the ZnO NP powder were recorded with a calibrated integrating sphere on FLS920 spectrometer.

Optical Materials EXPRESS

3. Results and discussion

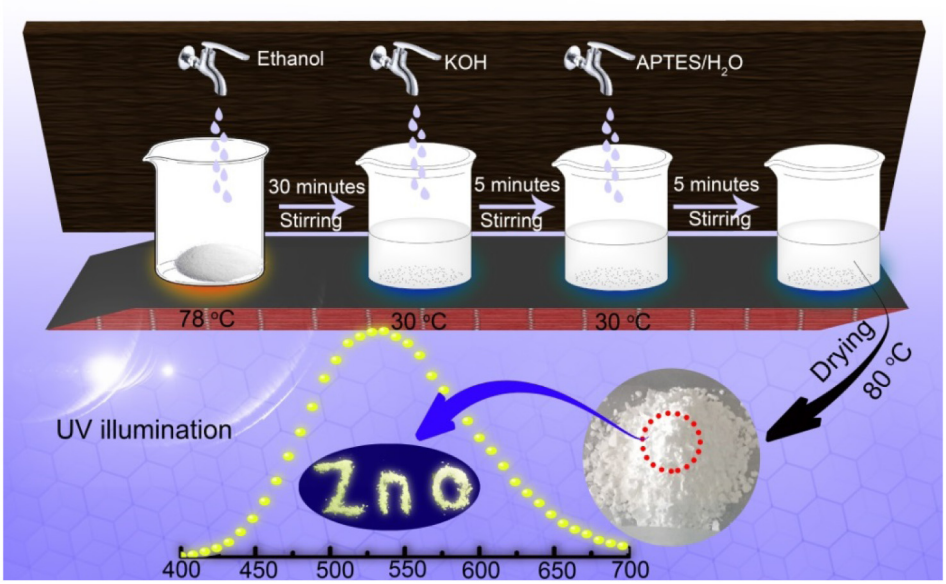

Fig. 1. Schematic illustration of the synthesis process of the ZnO NP powders.

The preparation process of the ZnO NP powders was elaborated in the experiment section, and the process is illustrated in Fig. 1. According to this method, over 34 g ZnO NP phosphors can be synthesized in one synthesis process, as shown in Fig. 2(a). The TEM image of the ZnO NPs shown in Fig. 2(b) reveals clearly that the NPs have a spherical shape with diameter of around 5 nm. Figures 2(c) and 2(d) are high-resolution transmission electron microscope (HRTEM) and selected area electron diffraction (SAED) pattern images of the NPs. The SAED pattern of the NPs shows several concentric rings, and lattice fringes with spacing of around 0.26 nm can be observed from the HRTEM image, which indicates the well-crystalline nature of the ZnO NPs. The size distribution of the ZnO NPs has been measured by dynamic light scattering analysis (DLS) method, as shown in Fig. 2(e). The mean size of the ZnO NPs is around 7.3 nm, which is roughly consistent with the TEM observations shown in Fig. 2(c) (about 5 nm). The XRD pattern of the ZnO NP powders is shown in Fig. 2(f). Some broad peaks appear in the pattern, which can be attributed to the diffraction of wurtzite ZnO. The small size of the ZnO NPs may be responsible for the relatively broad diffraction peaks. The bonding state analysis of the ZnO NPs characterized by XPS was indicated in Fig. 2(g), and the peaks of Zn 2P, O 1s, N 1s, C 1s and Si 1s can be observed from the pattern, in which the Zn 2P and O 1s peaks can be attributed to ZnO, while the peaks of N 1s, C 1s and Si 1s stem from surface modifier of (3-aminopropyl) triethoxysilane.

Optical Materials EXPRESS

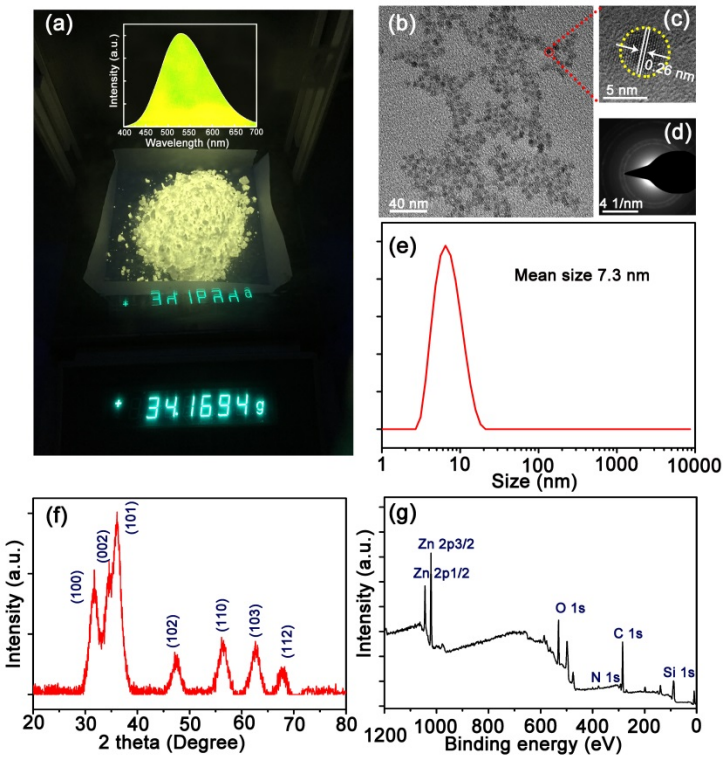

Fig. 2. (a) Image of the as-prepared ZnO NP powders. (b) TEM image of the ZnO NPs. (c) HRTEM image of the ZnO NPs. (d) Selected area electron diffraction pattern of the ZnO NPs. (e) DLS of the ZnO NPs. (f) XRD pattern of the ZnO NPs. (g) XPS spectrum of the ZnO NPs.

QY is a key factor that determines the figure-of-merit of phosphors, so the optical properties of the ZnO NPs were assessed. The fluorescence spectra of the ZnO NPs under different excitation wavelengths are shown in Fig. 3(a). All the fluorescence spectra of the NPs are dominated by a broad peak centered at around 535 nm, which can be attributed to the deep-level emission in ZnO [52, 53]. The photoluminescence excitation (PLE) spectrum at 535 nm has been measured, as shown in the Fig. 3(a). The PLE spectrum shows a sharp peak at around 370 nm. The QY of the ZnO NPs measured according to the literature [51] by FLS-920 is 42% and the corresponding images of the ZnO NP phosphors under UV lighting and indoor lighting conditions are shown in Fig. 3(b). The absorption edge of the ZnO NPs shown in Fig. 3(c) is located at around 370 nm, which stems from the near band-edge absorption of ZnO. To investigate the carrier recombination process of the ZnO NPs, transient photoluminescence spectrum of the ZnO NPs has been measured, as indicated in Fig. 3(d). The experimental data can be well fitted using the following two-order exponential decay formula:

$$y = y_0 + A_1 \exp(-t \ / \ \tau_1) + A_2 \exp(-t \ / \ \tau_2) \qquad (1)$$

where y is the emission intensity, y_0, A_1, A_2 are constant, t is time, and τ_1 and τ_2 are lifetime of the emission. The best fitting yields the lifetimes of τ_1 = 44.9 ns and τ_2 = 866.6 ns. Here τ_1 may come from the deep-level recombination inside the ZnO NPs; while $\tau 2$ may come from the surface defects [48, 49]. The inset of Fig. 3(d) is the schematic diagram of carrier recombination process.

Optical Materials EXPRESS

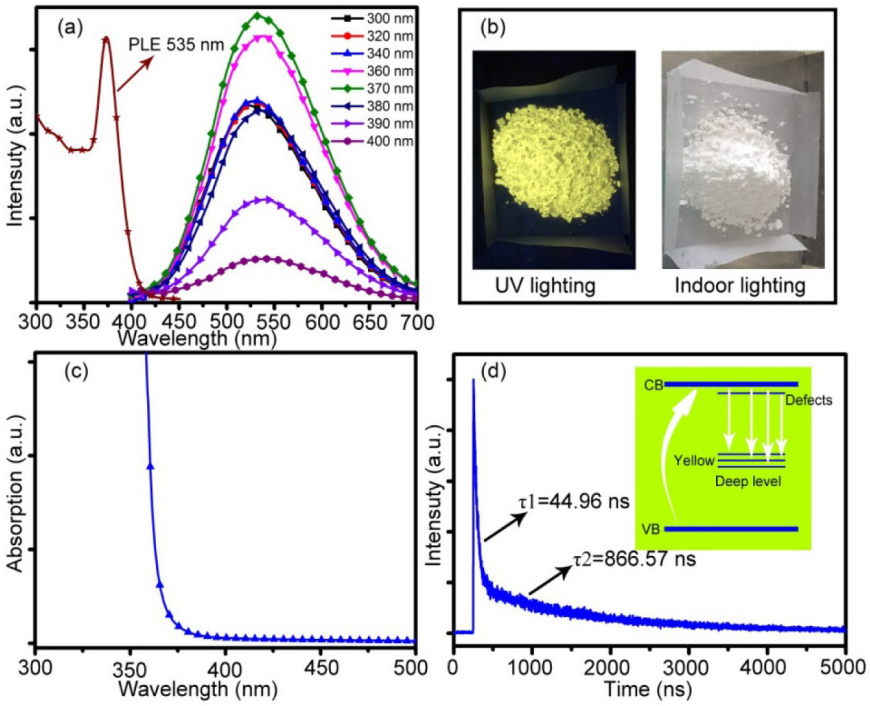

Fig. 3. (a) PLE spectrum at 535 nm and fluorescence spectra of the ZnO NPs under different excitation wavelengths. (b) Images of the ZnO NP powders under UV lighting and indoor lighting conditions. (c) Absorption spectrum of the ZnO NP powders. (d) Transient photoluminescence spectrum of the ZnO NPs, and the inset shows the schematic illustration of the carrier recombination process in the ZnO NPs.

To test whether the ZnO QDs can be employed as phosphors of LEDs, the ZnO NP powders were coated onto a UV LED chip. The emission spectrum of the UV chip is shown in Fig. 4(a), and for comparison, the PLE spectrum of the ZnO NP powders has also been listed in the Fig. 4(a). One can see that the emission spectrum of the UV chip accords well with the PLE spectrum of the ZnO NP powders, indicating that the ZnO NP powders can be excited efficiently by the UV chip. The electroluminescence (EL) spectra of the LED operated at different driving current ranging from 7.5 mA to 98.6 mA are also shown in Fig. 4(a). From the EL spectra, a broad emission peak centered at around 535 nm can be observed, and the emission intensity increases with the injection currents in our investigated range. The color coordinates change slightly from (0.35, 0.58) to (0.32, 0.48) when the injection current of the LED increases from 7.5 mA to 98.6 mA, as shown in Fig. 4(b). When the injection current is small, most the photons emitted from the UV chip can be absorbed by the ZnO NP phosphors to convert to visible emission, while with the increase of the current, some of the emitted photons cannot be absorbed by the ZnO NP phosphors, the proportion of the UV emission increases in the whole emission spectrum of the LEDs, leading to the shift of the color coordinate. The images of the LEDs under different injection currents are shown in Fig. 4(c), and bright yellowish luminescence can be observed from the device, which promises its application in lighting source.

Optical Materials EXPRESS

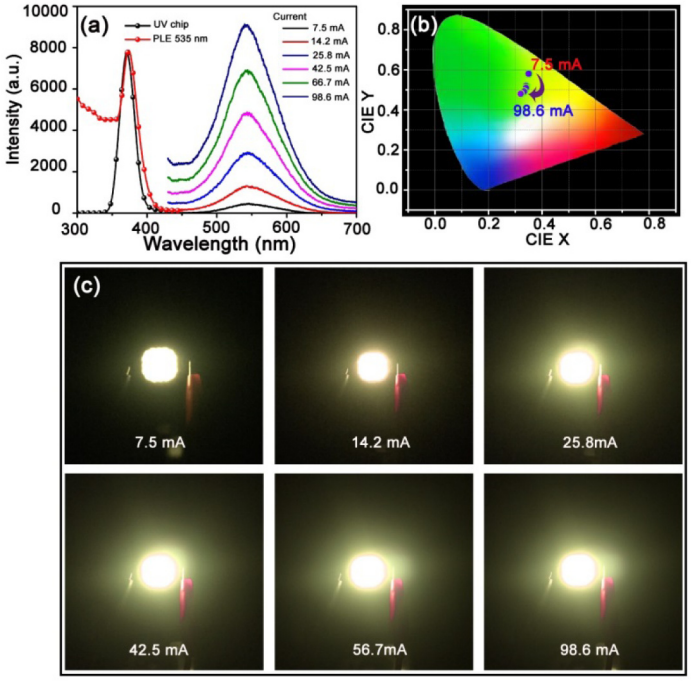

Fig. 4. (a) The emission spectrum of the UV chip, the PLE spectrum of the ZnO NP powders has also been illustrated for comparison, and the electroluminescence spectra of the UV chip coated with the ZnO NP phosphors operated at different injection current. (b) Color coordinate of the LED operated at different injection currents. (c) Images of the LED operated at different injection currents.

Table 1. The luminous efficiency of the LEDs under different driving current

Voltage(V)	Current (mA)	Optical powder density (mW/cm^2)	Visibility function factor	Luminous efficiency (lm/W)
9.0	7.5	4.4		40.5
9.1	14.2	11.3		54.1
9.2	25.8	23.5		61.6
9.3	42.5	40.8	0.91	64.2
9.4	66.7	56.2		55.7
9.5	98.6	72.2		47.9

The optical powder density of the LED (1×1 cm) under current from 7.5 mA to 98.6 mA is recorded by radiometers RM-12, and the corresponding luminous efficiency is calculated, as shown in Fig. 5(a). According to definition of light conversion efficiency, 1 W of optical power can convert to 683 lm at the wavelength of 555 nm. The luminous flux should be multiplied by visual function factor 0.91 at the wavelength of 535 nm in our study, and the detailed information can be seen in Table 1. The luminous efficiency of the LED can reach 64.2 lm/W when the injection current is 42.5 mA, which is much higher than that of common incandescent light bulbs (about 10 lm/W). The correlated color temperature (CCT) of the LED keeps at about 5200 K when it is operated at different injection current (Fig. 5 (b)), which is suitable for lighting. The stability of the emission color and CCT indicates that the LED can be employed as the lighting source. To test the stability of the LED further, the ZnO NPs were annealed at different temperatures for 30 min and the spectra of the LED have been recorded, as shown in Figs. 5(c) and 5(d). The luminescence intensity of the LED can maintain constant even the ZnO NPs are annealed at temperature as high as 100 °C, indicating the good temperature stability of the ZnO NP phosphors synthesized in our route.

Optical Materials EXPRESS

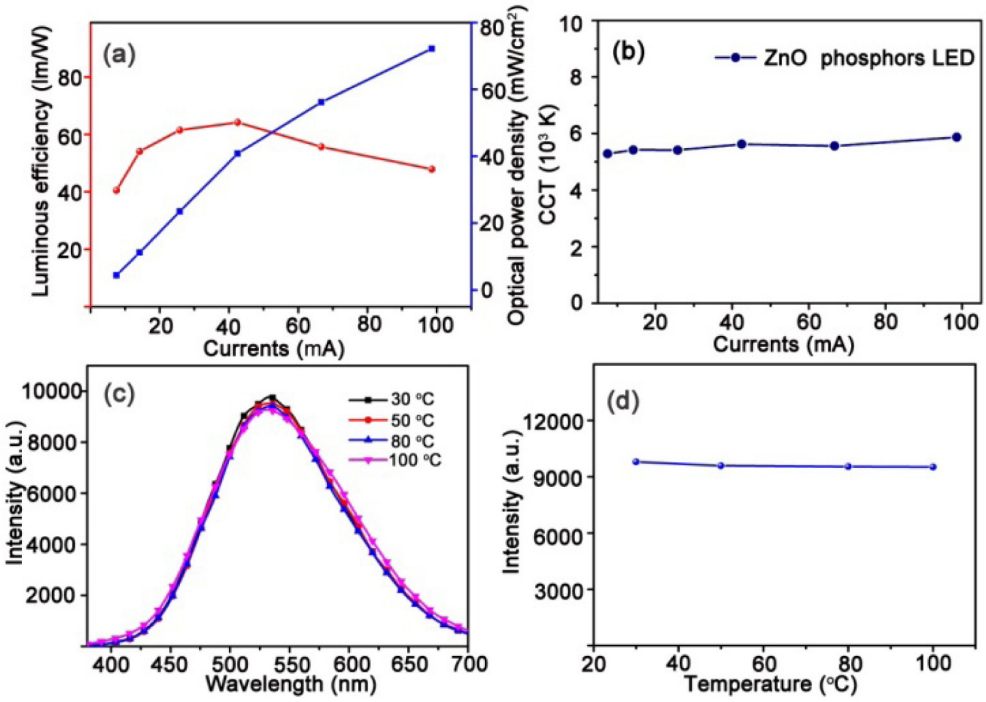

Fig. 5. (a) The luminous efficiency and optical power density of the ZnO NP phosphors coated LED. (b) CCT of the LED. (c) The luminescence spectra of the LED by coating ZnO NP powders treated with different temperatures. (d) The luminescence intensity of the LED coating ZnO NP powders treated with different temperatures.

4. Conclusions

In summary, a simple route to large-scale synthesis of ZnO NPs has been demonstrated, and the QY of the ZnO NP powders can reach 42%. The ZnO NP powders have been coated onto a UV LED chip as phosphors, and a yellowish LED has been realized. The luminous efficiency of the LED can reach 64.2 lm/W when the injection current is 42.5 mA. In addition, the luminescence intensity and CCT of the LEDs keep constant under different injection current, which can meet the requirements of bedroom lighting. Furthermore, the luminous intensity of the LEDs decreases little even when the ambient temperature reaches 100 oC, indicating the good temperature stability of the LEDs. The results reported in this paper demonstrate the application of ZnO NPs as the phosphors for LEDs for the first time, thus promise the future mass-application of ZnO NPs as low-cost and eco-friendly phosphors for LEDs.

Funding

National Science Foundation for Distinguished Young Scholars of China (61425021); National Natural Science Foundation of China (11374296, 21601159, U1604263).